FINITE ELEMENT ANALYSIS OF BOND SLIP BEHAVIOR IN PRETENSIONED BRIDGE GIRDER

Prashant Motwani, Research Scholar, Civil Engineering Department, IIT Bombay, Mumbai, INDIA
Arghadeep Laskar, Assistant Professor, Civil Engineering Department, IIT Bombay, Mumbai, INDIA

ABSTRACT

The transfer of prestress force from prestressing strands to the surrounding concrete is dependent on the bond between the two materials. It is essential to understand the actual bond stress distribution along the transfer length to determine the transfer zone in pretensioned concrete. Equations for estimating the transfer length in some codal provisions are based on the strand diameter only. The objective of this study is to examine the effects of excessive slip on strand development length and moment envelop of pretensioned bridge girders.

A 3-D nonlinear finite element model has been developed to simulate the transfer of prestress force from steel to concrete in pretensioned bridge girders. End slips were calculated from the Finite Element Model using a theoretical relationship proposed by Anderson and Anderson. Results obtained from the finite element analysis showed that the transfer length in the girders increases substantially due to the end slip of the strands. Investigation of the flexural behaviour of the bridge girder with varying strand surface conditions showed that the moment capacity of the girder with significant end slips is reduced in the development region. It can thus be concluded that, strand end slip measurement should be added to the quality control procedures for pretensioned members.

KEYWORDS: Bond Stress, Bridge Girder, End Slip theory, Finite Element Model, Pretensioned Concrete.

Notations

A_{ps}	Area of Prestressing steel, mm^2.
A_c	Area of Concrete, mm^2.
b	Power of Bond-Slip Relationship. [See Eqs. (16 and 17)].
d_b	Nominal Diameter of Prestressing Strand, mm.
d_c	Compression Damage Variable for Concrete.
d_t	Tension Damage Variable for Concrete.
E_c	Modulus of Elasticity of Concrete, MPa.
E_p	Modulus of Elasticity of Prestressing Strand, MPa.
$f_b(\xi)$	Bond Stress Distribution, MPa
f_{bo}	Initial Equi-biaxial Compressive Yield Stress, MPa.
f'_{ci}	Compressive Strength of Concrete at Transfer, MPa.
f_{co}	Initial Compressive Yield Stress, MPa.
$\frac{f_{bo}}{f_{co}}$	Ratio of Initial Equi-Biaxial Compressive Yield Stress to Initial Compressive Yield Stress.
f_{dev}	Developed Strand Stress, MPa.
f_{po}	Jacking Stress for Prestressing Strand, MPa.
f_{pu}	Ultimate Tensile Strength of Prestressing Strands, MPa.
f_{ps}	Ultimate Stress in Tendon, MPa.
f_{se}	Effective Stress in Prestressing Strand, MPa.
f_{si}	Initial Stress in Prestressing Strand, MPa.
k'	Dimensionless Coefficient which includes Parameters of the Bond-Slip Relationship, the Factor K_p and Concrete Strength. [See Eq. (18)].
K_p	Coefficient to Estimate Bond Stress Distribution. [See Eq. (19)].
k	Ratio of Second Stress Invariant on the Tensile Meridian.
k_m	Bond Stress Coefficient Matrix
l_b	Flexural Bond Length, mm.
l_t	Transfer Length, mm.
M_n	Nominal Moment Strength, kN-m.
n	$\frac{E_p}{E_c}$, Modular Ratio of Prestressing Strand.
P	Contact Pressure, MPa.

s_1	Slip Corresponding to Max Shear Stress, mm.
$s_{allowable}$	Allowable End Slip as per ACI Theory, mm.
s	Overall Slip of Tendon along the Transfer Length, mm.
$s(\xi)$	Variation of Slip along the Transfer Length.
t_m	Nominal Traction Stress Vector.
t_n	Normal (along the local 3 direction) Traction Stress.
t_s	Shear (along the local 2 direction) Traction Stress.
t_t	Shear (along the local 1 direction) Traction Stress.
x	Section Coordinate Measured from Stressed End when the Stress in Tendon reaches Effective Prestress, mm.
α	Coefficient Representing the Shape Factor of the Bond Stress Distribution along the Transfer Zone.
α_t	Coefficient of Thermal Expansion for Prestressing Steel, /^{0}c.
$\delta(\xi)$	Variation of Slip to Diameter ratio along the Transfer Length.
$\mathcal{S}$	$\frac{s}{d_b}$, Dimension Less Parameter.
δ_m	Contact Separation Vector
δ_n	Normal (along the local 3 direction) Separation.
δ_s	Shear (along the local 2 direction) Separation.
δ_t	Shear (along the local 1 direction) Separation.
Δ_{ps}	Total Elastic Shortening of Strand through Transfer Zone, mm.
Δ_c	Total Elastic Shortening of Concrete through Transfer Zone, mm.
ΔT	Change in Temperature, ^{o}c.
ε	Flow Potential Eccentricity.
ε^{el}	Elastic Strain Corresponding to Undamaged Material.
ε_c	Compressive Strain Corresponding to Compressive Stress, σ_c .
$\bar{\varepsilon}_c^{in}$	Inelastic Compressive Strains Corresponding to Stress Values.
$\bar{\varepsilon}_c^{pl}$	Compressive Plastic Strain in Concrete.
$\varepsilon_c(x)$	Concrete Strain after Transfer, Varying with Distance from End of Member.
ε_{pe}	Effective Prestress Strain in Strands after all Losses.
ε_{si}	Initial Steel Strain due to Prestressing Immediately Prior to Release.

$\varepsilon_s(x)$	Steel Strain after Transfer, Varying with Distance from End of Member.
ε_t	Tensile Strain Corresponding to Tensile Stress, σ_t .
$\bar{\varepsilon}_t^{in}$	Inelastic Tensile Strains Corresponding to Stress Values.
$\bar{\varepsilon}_t^{pl}$	Tensile Plastic Strain in Concrete.
Θ	$\frac{d_b{}^2\pi}{4A_{ps}}$, Equals to 1.287 for Seven Wire Strand.
μ	Viscosity Parameter.
μ_f	Coefficient of Friction between Strand and Concrete.
μ_s	Poisson's Ratio for Prestressing Steel.
μ_c	Poisson's Ratio for Concrete.
ξ	$\frac{x}{d_b}$, Non-dimensional Co-ordinate of the Section.
ρ_p	$\frac{A_{ps}}{A_c}$, Area Ratio.
σ_c	Concrete Compressive Stress Corresponding to Compressive Strain ε_c, MPa.
σ_t	Concrete Tensile Stress for Finite Element Modelling, MPa.
τ_{bf}	Ultimate Frictional Bond Resistance, MPa.
$\tau_{b\max}$	Maximum Bond Shear Stress, MPa.
$\tau_{\max}$	Maximum Shear Stress Corresponding to Slip s_1 to define ABAQUS Linear Traction Separation Law, MPa.
τ_{eq}	Equivalent Frictional Stress, MPa.
τ_{crit}	Critical Shear Stress, MPa.
ψ	Dilation Angle.

INTRODUCTION:

Prestress force in pre-tensioned concrete members is imparted through the bond stress between the strand and the concrete over the transfer length of the strand. The codal expressions for estimation of transfer length were experimentally developed from test results on 12.7 mm (0.5 in) diameter grade 1720 MPa (250 ksi), stress relieved strands. Based on these studies performed during 1950-1960, various codes namely Indian Standards (IS) [1], American Concrete Institute (ACI) [2] and the American Association of State Highway Transportation Officials (AASHTO) [3] recommended transfer length equations which are currently included in these codal provisions.

PRESENT CODAL PROVISIONS

The current codal provisions for transfer length of prestressing strand (contained in section 12.9 of ACI-318-14 [2]) are based on test results reported by Hansan and Kaar [4]. The transfer length has been derived using a transfer bond stress of 2.75 MPa (0.4 ksi) which represents the average value of bond stress obtained from tests conducted at the Portland Cement Association (PCA) for grade 1720 MPa (250 ksi) strands, The force equilibrium equation of a strand over the transfer length is given in Eq. 1.

$$\sum F_x = 2.75\left(\frac{4\pi d_b}{3}\right)l_t - 0.725\left(\frac{\pi {d_b}^2}{4}\right)f_{se} = 0 \quad (1)$$

The constant 0.725 in Eq. 1 is the ratio of actual area of grade 1720 MPa (250 ksi), 7-wire strand to the area of a circle of the same nominal diameter. The transfer length of the strand obtained from Eq. 1 is shown in Eq. 2, which is similar to the transfer length equation given in ACI 318-14 [2].

$$l_t = \frac{f_{se} d_b}{20.7} \quad (2)$$

It can be noted here, for grade 1860 MPa (270 ksi) strands, the ratio of the actual strand area to the area of the area of circle having same nominal diameter is 6 percent higher. Using the accurate area of the strands (as shown in Eq. 3) results in 8.4% higher transfer length as shown in Eq. 4.

$$\sum F_x = 2.75\left(\frac{4\pi d_b}{3}\right)l_t - 0.7685\left(\frac{\pi {d_b}^2}{4}\right)f_{se} = 0 \quad (3)$$

$$l_t = \frac{f_{se} d_b}{19.08}\text{(mm) or } l_t = \frac{f_{se} d_b}{3}\text{(in.)} \quad (4)$$

For an effective prestress, f_{se} of 1034 MPa (150 ksi) [3], Eq. 2 results in transfer length of $50d_b$, as given in Eq. 5, which is the approximate transfer length recommended in IS 1343 [1] and AASHTO [3] specifications.

$$l_t = \frac{1034\, d_b}{20.7} \cong 50 d_b \quad (5)$$

Eq. 2, is thus based on the transfer length of grade 1720 MPa (250 ksi), stress released strand of diameter 12.7 mm (0.5 in.) and concrete with bond stress of 2.75 MPa (0.4 ksi). However, newer low-relaxation strands have been introduced which requires revision of the present codal provisions. Eq. 2 considers effective prestress and strand diameter only in the calculation of transfer length in pre-tensioned members. However, comprehensive experimental and analytical studies by researchers (Rose and Russell. [5], Balazs [6], Jose et al. [7], Hwan al. [8], Dang et al. [9]), have showed that, the transfer length is also dependent on type of tendon, concrete strength, concrete cover , bond condition, type of release and surface condition.

FUNCTION OF BOND

Considerable research on the bond between prestressing strands and concrete has been reported in the literature. Janney [10] was one of the earliest pioneers to investigate the physical characteristics of bond between prestressing strands and concrete and its relationship to the transfer and development lengths of the strands. Janney [10] concluded that the bond between the prestressing steel and the surrounding concrete is dependent on 3 major factors; namely adhesion due to glue like property of cement , friction between concrete and steel and mechanical resistance due to the interlocking of the spiral twisting of the wires forming the strand with the surrounding concrete. Adhesion is only present if no slip exist between strands and concrete. However, the strain differentials between strands and concrete suggest that slip is inevitable and thus adhesion contributes minutely to prestress bond. Mechanical interlock is not a dependable bond mechanism for prestress transfer in pre-tensioned members (Marin and Scott [11]). Therefore, friction is considered to be the principal contributing factor to the stress transfer from prestressing steel to concrete. Frictional forces between the strands and the surrounding concrete develop due to the high radial pressure exerted against the concrete by the strands, which tend to expand diametrically during the transfer of prestress forces (Fig. 1). This results in transfer of prestress from steel to concrete as explained by Galvez et al. [12].

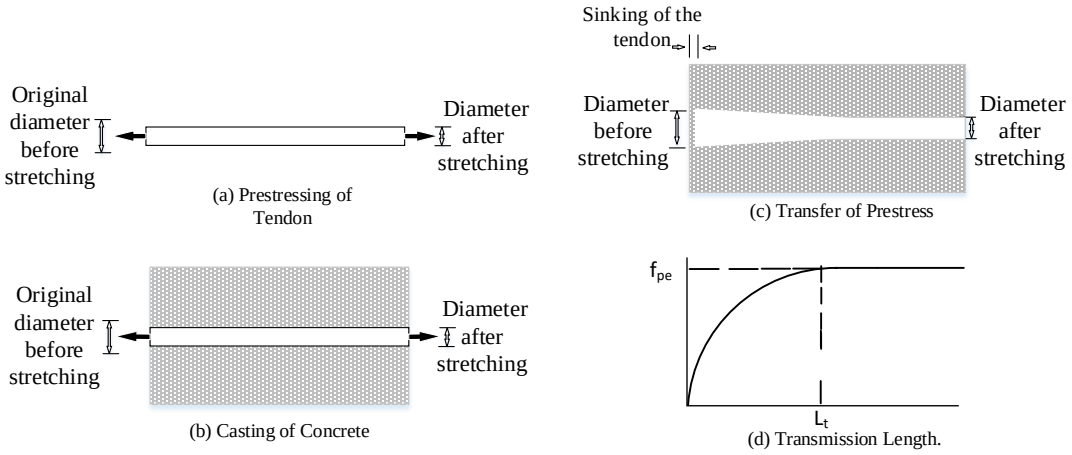

Fig 1Transfer of Prestress as per Hoyer's Effect

In recent years, extensive experimental studies have been carried out to characterize the bond behavior of pre-tensioned members. Three of the most significant studies to test the bond behavior in pre-tensioned members consisted of the pull-out tests by Moustafa [13], bond tests by Post-tensioning Institute (PTI) [14] and North American Strand Producers (NASPs) [15]. According to recent studies, the PTI bond tests are the most accurate representation of the bond capacity of prestressing strands. [15].

Research conducted by Uijl [16] showed that the bond stress of prestressing strands decreases linearly over the transfer length. In particular, the bond stress is maximum near the free end of pre-tensioned beam, due to poisson's effect and decreases along the transfer length. However it should be noted that Eq. 2, had been developed assuming a constant bond stress of 2.75 MPa (0.4 ksi) along the transfer length.

STRAND SLIPPAGE

When tendons are cut to transfer the prestressing forces to concrete members, they tends to move in same direction in which the prestressing force is applied to concrete. The relative movement of the strand with respect to the surrounding concrete is prevented by the bond between the two materials. If the bond is inadequate to prevent the relative movement between the strands and the surrounding concrete, a bond failure will occur because of excessive slippage of the prestressing strand, as shown in Fig 1(c). ACI 318-14 [2] codal provisions specify that the quality assurance procedures for pre-tensioned applications should be used to confirm that the bond properties of concrete and the reinforcement are adequate. However, there are no minimum requirements for the bond performance between concrete and steel in ACI 318-14 [2] or in standards like ASTM [17]. If slip is absent, the reduction in tensile strain occurring in steel at any point following the release of pretension must be equal to the increase in compressive strain in the concrete at the same point. Measured strains indicate that the strain compatibility conditions are effective only in the central portion of the members where the tension in the strands is constant [10], as shown in Fig 1(d).

Anderson and Anderson [18] observed that the reduction in steel strain is greater than the corresponding increase in concrete strain within the transfer zone of the strands. The difference between the steel and concrete strains increases as the steel stress gradient increases. Prior to the release of the prestressing force, the strands are tensioned to a stress f_{si}. Following the transfer of prestressing force to concrete, the tension drops to zero at the end of member and to f_{se} at the end of transfer zone. The

corresponding change in steel strain ranges from $\frac{f_{si}}{E_p}$ at the end to $\frac{f_{si} - f_{se}}{E_p}$ at a distance equal to transfer length (Fig 2).

Since the concrete strain changes from 0 to $\frac{f_{si} - f_{se}}{E_p}$ over the transfer zone in the same sense as the change in steel strain, there is a differential strain change between the two materials varying from $\frac{f_{si}}{E_p}$ at the end to zero at the end of transfer zone. This change in differential strain through the transfer zone as shown in Fig 2 results in cumulative relative displacement between the steel and concrete over the transfer length. Based on the above fundamental mechanics and strain compatibility, a theoretical relationship for end slip of prestressing strand was proposed by Anderson and Anderson [18] as shown in Eq. 6.

$$s = \Delta_{ps} - \Delta_c$$
$$s = \int_0^L \{\varepsilon_{si} - \varepsilon_s(x)\}dx - \int_0^L \varepsilon_c(x)dx \quad (6)$$

The end slips have been indirectly used to estimate transfer length by various researchers ([5], [6], [7], [8], [9]). Guyon [19], proposed an expression to estimate transfer length from end slip (Eq. 7).

$$l_t = \alpha \frac{s}{\varepsilon_{si}} \quad (7)$$

Guyon [19] considered two different hypothesis to calculate the value of α in Eq. 7; namely constant bond stress hypothesis and linearly descending bond stress hypothesis. In constant bond stress hypothesis, the strand stress is assumed to be linearly increasing along the transfer length, as shown in Fig 2a. In case of linearly descending bond stress hypothesis, the stand stress is assumed to have a second order variation along the transfer length, as shown in Fig 2b

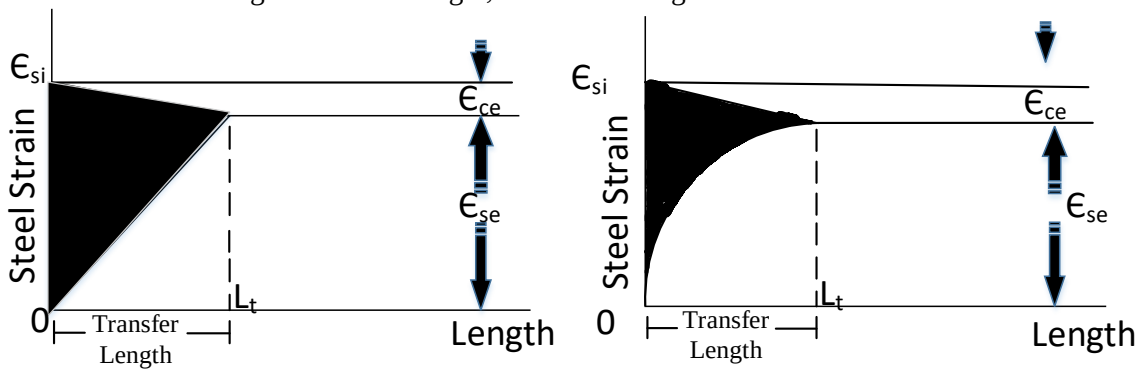

(a) Constant Bond Stress Hypothesis (b) Linearly Decreasing Bond Stress Hypothesis

Fig 2 Bond Stress Hypothesis

Extensive studies have been performed by various researchers to propose different values of α for different bond stress distribution along the transfer length. Guyon [19] proposed α values of 2 and 3 for constant bond stress hypothesis and linearly descending bond stress hypothesis respectively. However, comprehensive experimental studies by Jose et al. [7] and Uijl [16], have showed that, α should be 2.44 and 1.5 respectively.

BOND STRESS SLIP RELATIONSHIP

The prestressing force is transferred from the strands to the concrete by the bond stresses which are activated by the slips at the interface between concrete and steel. The bond stress between the concrete and the strand have been previously correlated to the strand slips for a given concrete grade (Jose et al. [7]), concrete cover (Bamonte et al. [20]) and diameter of bar (Stephen [21]). Considering stress equilibrium and strain compatibility conditions along with elastic behavior of steel and concrete and assuming bond-slip behavior given in Eq. 8 over the transfer length, Balazs [6] developed nonlinear equations for slip distribution (Eq. 9) over transfer length as shown in Fig. 3a.

$$f_b = c\sqrt{f'_{ci}}\,\delta^b \tag{8}$$

$$\delta(\xi) = \frac{s(\xi)}{d_b} = k'\xi^{\frac{2}{1-b}} \tag{9}$$

The parameters c and b in Eqs. 8 and 9 are experimental constants assumed to be 2.055 MPa (0.783 ksi) and 0.25 respectively for 12.7 mm (0.5 in.) seven wire strand [6]. Therefore the constants k' and ratio 2/(1-b) for 12.7mm (0.5 in.) 7 wire strand can be written as shown in Eqs. 10 through 12.

$$\frac{2}{1-b} = \frac{8}{3} \tag{10}$$

$$k' = 0.357\sqrt[3]{K_p{}^4 f'_{ci}{}^2} \tag{11}$$

$$K_p = 5.15\frac{(1+\mathrm{n}\rho_\mathrm{p})}{\mathrm{E_p}} \tag{12}$$

Balazs [6] also proposed an equation for bond stress distribution as given in Eq. 13 and schematically shown in Fig 3b.

$$f_b(\xi) = 0.8904\left[5.15\frac{(1+\mathrm{n}\rho_\mathrm{p})}{\mathrm{E_p}}\,f'_{ci}{}^2\right]^{1/3}\xi^{2/3} \tag{13}$$

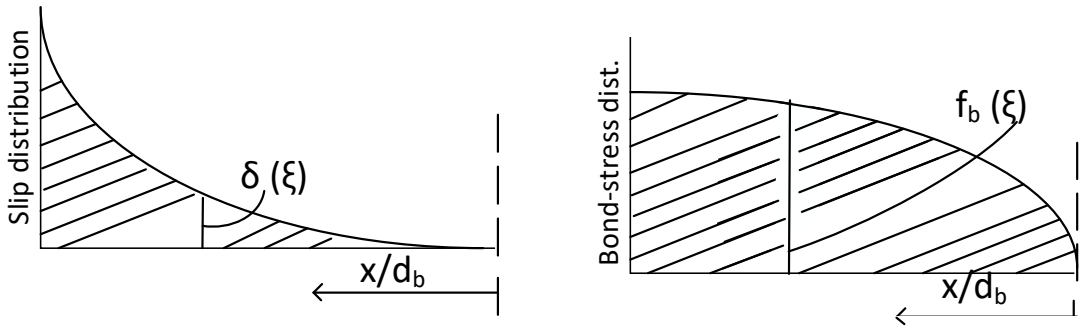

(a) Slip Distribution over Transfer Length (b) Bond Stress Distribution over Transfer Length

Fig 3 Schematic Diagrams for Analytical Equations Proposed by Balazs [6]

FINITE ELEMENT ANALYSIS OF PRETENSIONED MEMBERS

Various finite element models have also been developed by researchers over the past decade to study the nonlinear behavior of pre-tensioned prestressed bridge girders. Stephen [21] utilized ABAQUS commercial software to simulate long term behavior of pre-tensioned bridge girders. Long term effects like creep and shrinkage were implemented in the model using an elastic-plastic material model. In order to facilitate operations like creep and application of prestress, subroutine files were written in FORTRON-90. Kannel et al. [22] developed three-dimensional finite element model to investigate the effect of release methodologies on the end cracking in pre-tensioned concrete. The transfer length was modelled by varying the cross sectional area of the strands linearly from zero at the ends of the girder to the maximum at the end of theoretical transfer length. A non-linear finite element model was analyzed

using ANSYS software by Motwani et al. [23] to analyze railway prestressed sleepers. The model included three dimensional 8 noded brick elements to model the concrete matrix and one dimensional truss element to model prestressing strands.

From the literature, it can be well understood that over the past few decades, researchers have conducted numerical, analytical and experimental studies on the bond stress-slip behavior in pre-tensioned members as it is significant in the estimation of the transfer length of the strands.

A lot of experimental work has been done in the past to investigate the effect of various parameters on the transfer length and end slip of pretensioned strands. These experimental investigations required significant amount of time and money. Considering the significant difference between the experimental and computational cost and time, finite element analysis can be more feasible and economical with a reasonable level of accuracy. Therefore, the aim of this study is to develop an extensive finite element model that accounts for different bond stress-slip relationships to estimate the transfer length. In this paper a robust, three-dimensional nonlinear finite element model has been developed to simulate the transfer of prestressing forces from steel to concrete in pre-tensioned bridge girders. End slips obtained from the model for varying strand surface conditions have been validated using a theoretical relationship proposed by Anderson and Anderson [18]. Moment envelop and developed stress envelop were obtained using the simulation results and studied for changing surface conditions of the strands and surrounding concrete.

EVALUATION OF END SLIPS AND TRANSFER LENGTH FROM FINITE ELEMENT ANALYSIS

OUTLINE OF ANALYSIS

The transfer of prestress from steel to concrete through Hoyer effect explained by Galvez et al. [12] leads to lateral expansion of tendons resulting in circumferential tensile stresses in concrete. This tensile stresses may cause cracking in concrete around the tendon. This phenomenon may not be well simulated using two-dimensional analysis. Hence three-dimensional analysis has been implemented in this study to accurately simulate the transfer of prestressing forces from tendons to concrete. The finite element model presented in this research has been developed using ABAQUS finite element analysis software [24].

The developed finite element model has been validated using the test results of a TxDOT Type-A bridge girder tested by Laskar et al. [25]. The girder was prestressed using twelve, grade 1860 MPa (270 ksi), low-relaxation strands of 12.7 mm (0.5 in.) diameter and was tested under four point loading scheme. The schematic layout of the beam tested by Laskar et al. [25] is shown in Fig 4.

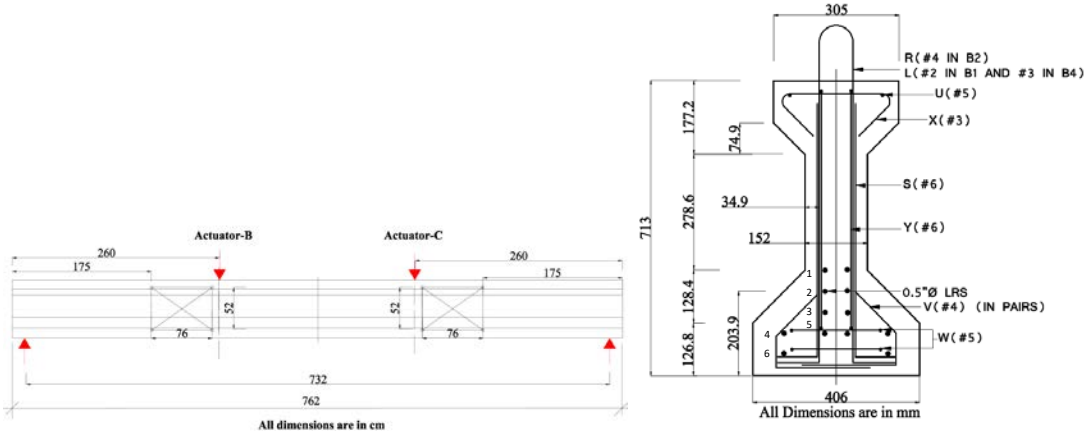

Fig 4 Loading Positions and Cross-Section of Bridge Girder Tested by Laskar et al. [25]

Symmetry of the structure has been utilized and only one-fourth of the girder was modelled in ABAQUS as shown in Fig 5.

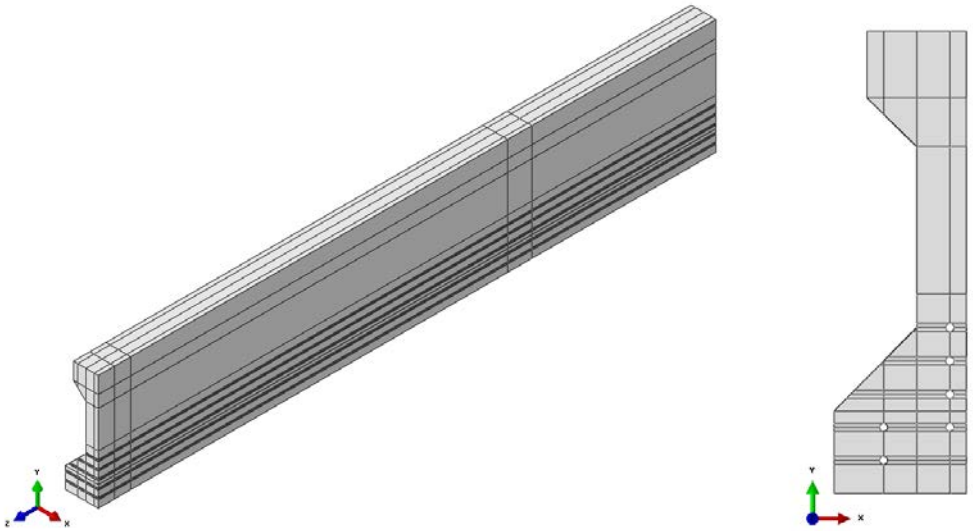

Fig 5 3D FE Model of Beam Tested by Laskar et al. [25]

CONSTITUTIVE MODELS FOR CONCRETE AND STRANDS

The constitutive relationships of concrete in compression and tension were modelled using the nonlinear stress-strain curves proposed by Carreeira and Chu [28, 29] (Figs 6 and 7).

CONCRETE COMPRESSION MODEL

The elastic-plastic response of concrete has been modelled using the concrete damage plasticity (CDP) model proposed by Lee and Fenves [26]. The concrete damage is represented in the CDP model using a combination of multi-hardening plasticity and scalar (isotropic) damaged elasticity. The default parametric values for ψ, ε, k, μ and $\frac{f_{bo}}{f_{co}}$ obtained from ABAQUS Theory Manual [27] has been used to define the CDP model in this study.

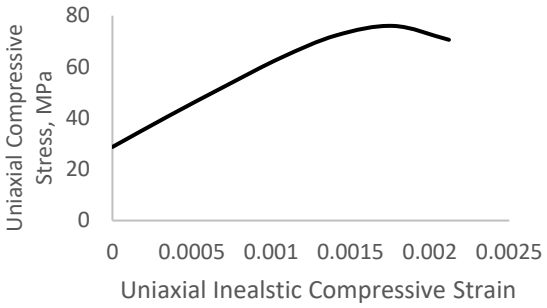

Fig 6 Uniaxial Stress-Strain Curve of Concrete in Compression [28]

The non-linear stress-strain relationship of concrete under compression has been defined by specifying the values of uniaxial compressive stresses (σ_c) corresponding to uniaxial inelastic strain $(\bar{\varepsilon}_c^{in})$ and damage variable (d_c) in the post-peak region. The damage variable (d_c) is utilized to define the damaged response of the concrete model and is calculated using Eq. 14.

$$d_c = 1 - \frac{\text{Compressive Stress at Undamaged Path}}{\text{Compressive Stress at Peak}} \tag{14}$$

The total strain values in concrete (ε_c) have been converted into inelastic strains using Eqs. 15 and 16.

$$\bar{\varepsilon}_c^{in} = \varepsilon_c - \varepsilon^{el} \tag{15}$$

Where, $$\varepsilon^{el} = \frac{\sigma_c}{E_c} \tag{16}$$

The plastic strain values $\bar{\varepsilon}_c^{pl}$ calculated using Eq. 17 were manually eliminated if they were either negative or decreasing with increased stress values to avoid convergence errors [27].

$$\bar{\varepsilon}_c^{pl} = \bar{\varepsilon}_c^{in} - \frac{d_c}{1-d_c}\frac{\sigma_c}{E_c} \tag{17}$$

CONCRETE TENSION MODEL

The constitutive relationships of concrete in tension has been defined by specifying the values of tensile stress (σ_t), cracking strain $(\bar{\varepsilon}_t^{in})$ and damage parameter (d_t) in tabular form. The damage parametre d_t is defined similar to d_c with compressive stress replaced by tensile stress, as defined in Eq. 14. The ineleastic strain has been calculated from the total strain (ε_t) using Eq. 18.

$$\varepsilon_t^{in} = \varepsilon_t - \varepsilon^{el} \qquad \text{Where, } \varepsilon^{el} = \frac{\sigma_t}{E_c} \tag{18}$$

Similar adjustments as shown in Eq.17 have has been performed to ensure tensile plastic strains $(\bar{\varepsilon}_t^{pl})$, are neither negative nor decreasing with increasing tensile stress value.

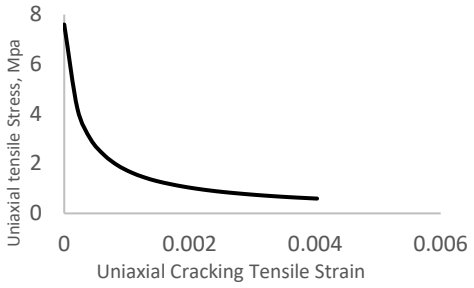

Fig 7 Uniaxial Stress-Strain Curve of Concrete in Tension [29]

STRAND MODEL

The prestressing strand of grade 1860 MPa (270 ksi) has been stressed to a maximum value of $f_{po} \le 0.75 f_{pu}$ commonly known as jacking stress. The effective prestress imparted to strands was 1007 MPa. The nonlinear stress-strain curve for the prestressing strands used in the finite element model (as shown in Fig 8) has been derived from the experimental stress-strain data of the strands (Wang [30]). Inelastic strains in the non-linear stress-strain curve were derived from the experimental strains using Eqs. 15 and 16.

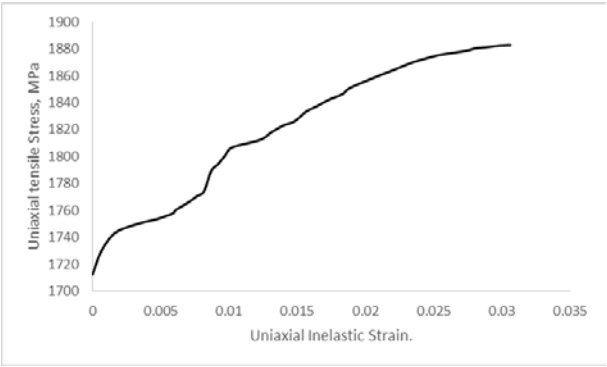

Fig 8 Uniaxial Stress-Strain Curve of Strands

INTERFACE MODELLING

The interaction between strand and concrete is simulated using contact formulation. This is facilitated by modelling concrete as well as strands as a solid continuum using eight noded reduced integration brick elements and six noded triangular elements respectively. Concrete is extruded along the six strand locations and strands are modelled on the extruded concrete surface. An extruded model requires contact properties in order to model the composite action between strand and concrete including slippage, friction, and temperature dependency.

TANGENTIAL BEHAVIOR

The tangential behavior of the contact surfaces is represented by the coefficient of friction μ_f in the developed finite element model. The standard coulomb friction model assumes that no relative motion occurs if the equivalent frictional stress, τ_{eq} is less than critical stress, τ_{crit} given in Eq. 19. The value of coefficient of friction μ_f used in the finite element model is 0.55 based on recommendations of AASHTO LFRD Bridge Design Specification [31]. Eq. 19 gives the limiting frictional shear stress for the contacting surfaces. There is no relative displacement between the strands and concrete if the shear stress is less than τ_{crit}.

$$\tau_{crit} = \mu_f P \tag{19}$$

The solid line in Fig 9 summarizes the behavior of the Coulomb friction model. There is zero relative displacement (slip) of the surfaces when they are "sticking" (the shear stresses are below τ_{crit}).

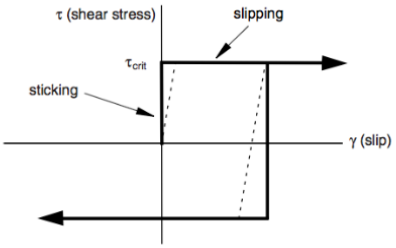

Fig 9 ABAQUS Penalty Friction Model [27]

In ABAQUS/Standard the discontinuity between the two states of sticking or slipping can result in convergence problems during the simulation. Therefore, a penalty friction formulation with an allowable elastic slip, has been adopted as shown by the dotted line in Fig 10. ABAQUS automatically calculates the penalty stiffness and ensures that the allowable elastic slip does not affect the accuracy of the simulation model.

COHESIVE BEHAVIOR

The interaction between two surfaces can be simulated in ABAQUS by using either the cohesive elements approach or the surface-based cohesion approach. When the interface thickness is negligible, surface-based cohesion approach is recommended for its convenience and effectiveness. If the interface adhesive layer has a finite thickness and macroscopic properties (such as stiffness and strength) of the adhesive material are available, it is more appropriate to model the response using cohesive element approach. Since interaction between tendon and concrete does not have any interface layer therefore cohesive surface based approach has been utilized for the present analysis.

The stress-slip relation proposed by Eligehausen et al. [32] has been considered as the theoretical basis for the modelling of the tendon-concrete cohesive behaviour in ABAQUS. Fig. 10a shows the bond-slip model proposed by Eligehausen et al. [32], where the initial penetration of the ribs into the mortar matrix is represented with the ascending part, up to a maximum stress $\tau_{b\max}$, followed by a plateau only for confined concrete. Finally, the descending part marks the beginning of shearing of the concrete due to the ribs of reinforcement bar. The bond stress continues to decrease until a constant

residual stress of τ_{bf} is reached. This residual bond stress is due to pure friction between the reinforcement bar and the surrounding cracked concrete.

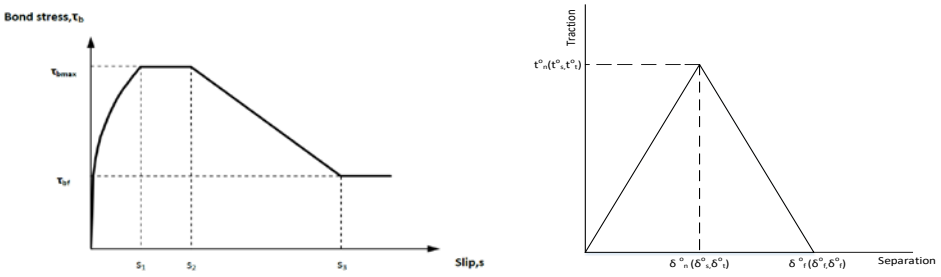

(a) Model by Eligehausen et al.[32] (b) ABAQUS Idealised Model [27]

Fig 10 Bond Stress-Slip Modes

ABAQUS assumes linear traction-separation behaviour, as shown in Fig 10 (b), which relates normal and shear stresses to the normal and shear separations across the interface before the initiation of damage.

The nominal traction stress vector, t consists of three components t_n t_s and t_t. The corresponding separation is denoted by δ_n, δ_s and δ_t respectively. The traction separation matrix shown in Eq. 20 provides coupled behaviour between all components of the separation vector and traction vector.

$$t_m = \begin{bmatrix} t_n \\ t_s \\ t_t \end{bmatrix} = \begin{vmatrix} k_{nn} & k_{ns} & k_{nt} \\ k_{ns} & k_{ss} & k_{st} \\ k_{nt} & k_{st} & k_{tt} \end{vmatrix} \begin{bmatrix} \delta_n \\ \delta_s \\ \delta_t \end{bmatrix} = k_m \delta_m \tag{20}$$

By default, the normal and tangential stiffness components will not be coupled as pure normal separation by itself does not give rise to cohesive forces in the shear directions, and pure shear slip with zero normal separation does not give rise to any cohesive forces in the normal direction. Thus it was decided to use uncoupled traction separation law which requires defining only the diagonal terms of the traction separation matrix shown in Eq. 20.

According to Gan [33], the bond stress coefficients k_{nn} and k_{tt} are obtained by approximation of the bond-slip relationship. The stiffness of the normal traction is taken as 100 times the stiffness of the shear traction as shown in Eq. 21.

$$k_{ss} = k_{tt} = \frac{\tau_{\max}}{s_1} \text{ N/mm}^3$$
$$k_{nn} = 100 k_{ss} \text{ N/mm}^3 \tag{21}$$

For the present study multiple bond stress-slip relationships have been considered by using different values of bond stress coefficient (k_{tt} and k_{ss}) in order to simulate the varying surface condition of strands. Herrero et al. [34] reported peak bond stress of 5.3 MPa (0.76 ksi) and corresponding slip as 0.8 mm (0.03 in.), as shown in Fig 11. Using Eq. 21, k_{ss} and k_{tt} have been obtained as 6.66 N/mm (0.038 ksi/in.) and k_{nn} as 666.66N/mm (3.80 ksi/in.). Table 1, gives the values of bond stress coefficients (k_{tt} and k_{ss}) used in the various cases analysed using the finite element model in this study. The bond stress coefficients obtained through push-in bond tests performed by Herrero et al. [34] have been utilized as a reference to simulate the cohesive behaviour between strands and surrounding concrete. Therefore bond stress coefficients used in Case 4 represents a realistic case and could be expected in a normal girder.

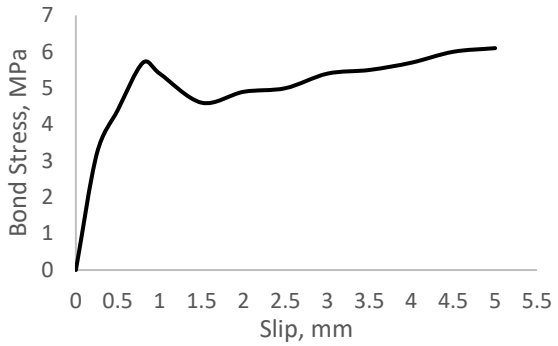

Fig 11 Bond Stress-Slip Relation Proposed by Herrero et al. [34]

Table 1 Nomenclature for the FE model and their respective Bond Stress Coefficients.

Nomenclature	Case 1	Case 2	Case 3	Case 4	Case 5	Case 6	Case 7
Bond Stress Coefficient, N/mm^3	1.370	2.000	3.330	6.660	8.000	26.64	266.0

Note: 1 N/mm^3= 5.71e-3 Kips/in^3.

SIMULATION OF PRESTRESS

The prestressing of tendons has been simulated by applying a thermal load (temperature decrease) in the tendons based on the relation between strain change and temperature change (Chen et al. [35]). The prestressing force in the tendons could not be implemented by applying a pre-defined strain on the tendons due to convergence problems caused by the development of high stresses in the surrounding concrete near the two ends of the tendons. The strain change due to the applied prestress in the tendons has been related to the thermal strain change due to the applied thermal load in the tendons as shown in Eq 22.

$$f_{se} = E_p \varepsilon_{pe} \quad \text{MPa}$$
$$f_{se} = E_p (\alpha_t \Delta T) \text{ MPa} \tag{22}$$

The thermal load (temperature change) to be applied to the tendons has been calculated using the jacking prestress and considering total prestress losses to be 25% as per AASHTO guidelines [3].

RESULTS AND DISCUSSIONS

Load deformation response

In order to validate the proposed model, load deflection response of case 4 has been compared to the experimental results reported by Laskar et al. [25] as shown in Fig. 12.

On comparing the experimental load-deflection responses with finite element prediction, it can be observed that the results match perfectly in the linear range. However, considerable difference between the experimental and analytical results can be observed in the non-linear range. The difference in the experimental and predicted non-linear responses was not minimized since most of the results reported in the present study are due to application of prestressing force prior to the application of external loads. Thus the results from the finite element analysis used in the present study are corresponding to the linear response of the girder. The only result taken from the loading step (Step 2) was the ultimate stress which has been over-predicted to some extent from the finite element analysis. The experimental failure load of the analyzed girder was 430kN (97 kips). The peak load obtained from the finite element model was 495 kN (111.2 kips). The maximum compressive strain in concrete at the peak load was 0.00414 from the analysis results. Furthermore, the ultimate tendon stress f_{ps} at the peak load of 495kN (111.2 Kips) was 1710 MPa (248 ksi).

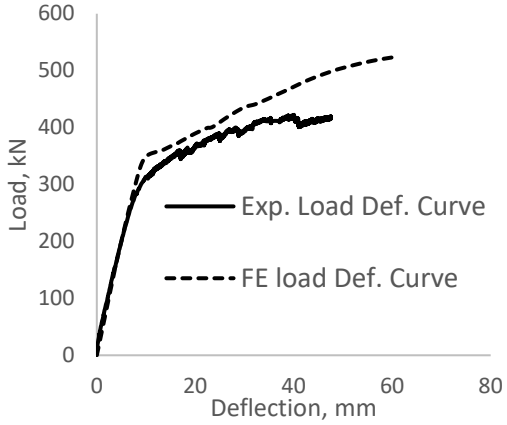

Fig 12 Comparison of Experimental and Finite Element Load Deflection Curves

Bond Stress Distribution and Slip Distribution

The bond stress and slip distribution proposed by Balazs [6] reported in Eqs. 9 and 13 respectively (schematically shown in Fig 3a and 3b) , have been utilized to qualitatively compare the finite element bond stress and slip distribution for Case 4 and is shown in Figs. 14a and 14b, respectively. The pattern of bond stress and slip distribution proposed by Balazs [6] and obtained from the finite element analysis results (Fig. 13) match qualitatively with the distributions proposed by Balazs [6] as shown in Fig. 3.

It has been observed from the nonlinear finite element analysis results that with same initial prestress defined for all strands, the effective prestressing force from strand 1 to 6 (Fig 4) vary from 1007 MPa to 987 MPa. This decrease in prestress has been identified due to the elastic shortening of concrete which is maximum at the bottom most strand location and minimum at the top strand location closest to the c.g. of the girder. Since the bond stress and hence the tendon slip are dependent on the push in force, the bond stress and slip distribution showed variation at different strand location as shown in Fig 6. This serves as an additional validation for the finite element model.

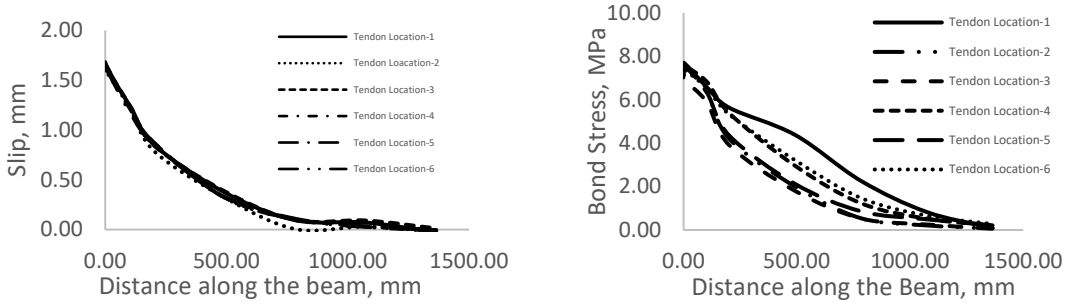

(a) Slip Distribution (b) Bond Stress Distribution

Fig 13 Bond Stress and Slip Distribution for Case 4

Transfer Length

In the present study, the transfer length of the tendons has been predicted using a similar approach of 95% of the average maximum strain (95% AMS) as recommended by Russell and Burns [36]. Rather than calculating the maximum strain along the girder, 95% of the average maximum stress along a strand was calculated. The transfer lengths obtained for all the cases (representing different strand and concrete surface conditions) analysed in this study are shown in Fig 14. The average transfer lengths of the six tendons of the girder (Fig. 4) obtained for the various cases studied through the finite element analysis have been compared with codal provisions of IS [1], ACI 318-14 [2] and AASHTO [3] as well as with transfer lengths proposed by other researchers. The results of the comparative study are shown in Table 2.

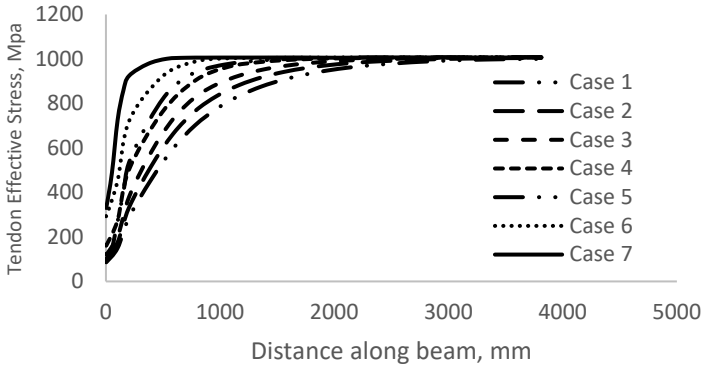

Fig 14 Variation of Transfer Length with Strand Concrete Surface Conditions in FE Model

Surface Roughness of Prestressing Steel

The bond between strands and concrete improves with increase in roughness of strands (Barnes et al. [36]). The bond stress-slip coefficients in the model was varied between 1.37 N/mm^3 (7.79 x 10^{-3} kips/in.^{3}) to 2664 N/mm^3 (1520.86 x 10^{-3} kips/in.^{3}) (Table 1) to investigate the influence of surface roughness.

Fig. 15 shows that finite element models with a higher bond stress coefficient have smaller transfer length in comparison to those with lower bond stress coefficient. Similar finding was also reported by Cousins et al. [38]. It can also be observed in Fig. 14 that the tendons in all the finite element models developed same effective stress level, showing that the surface roughness has no influence on the effective prestress f_{se}.

Strand Slipping

The initial slip is a direct indication of the bond quality. The slip is therefore directly related to transfer length (Guyon [19]). Slip theory, proposed by Anderson and Anderson [18], (Eq. 6) has been utilized in this study to calculate the slippage of the strands from the analysis results. A linear regression analysis has been performed on 42 values of transfer length and end slip obtained from the seven cases analyzed in this study (Fig. 15) to propose the relationship of transfer length and end slip of the strands as shown in Eq. 23

$$l_t = 266.6s \text{ mm} \tag{23}$$

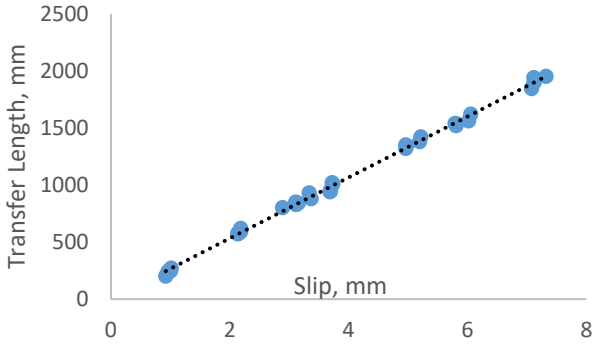

Fig 15 Relationship between End Slippage and Transfer Length of Simulated Bridge Girder

The transfer lengths of the strands obtained from the proposed relationship between transfer length and end slip of the strands has been compared with available literature (Rose and Russell [5], Balazs [6], Jose et al. [7], Hwan et al. [8], Moustafa [13]) correlating transfer length with strand slippage, as shown in Table 5. Another transfer length equation proposed by Barnes et al. [37] which is independent of end

slip has also been utilized for comparison. It can be seen from Table 2 that the transfer lengths calculated from the proposed relationship agree well with the transfer lengths obtained from literature. However the calculated transfer length are significantly lower when the strand slippage is not considered as in the codal provisions as well as by Barnes et al. [37].

Table 2 Comparison of Transfer Lengths from FEA Results with Codal Provisions and Recommendations by other Researchers.

Case	Avg slip from FEM (mm)	Avg f_{se} from FEM (MPa)	Calculated Transfer Length										
			Predicted Eq. 23 from FE Result (mm)	Avg. L_t from FEM (mm)	Codal Provisions			Literature					
					ACI (mm)	AASHTO (mm)	IS (mm)	Rose and Russell [5] (mm)	Balazs [6] (mm)	Jose et al. [7] (mm)	Hwan et al. [8] (mm)	Guyon [13] (mm)	Barnes et al. [37] (mm)
Case 1	7.15	993	1907	1911	609	635	381	2136	2088	2438	1648	1999	352
Case 2	5.88	993	1568	1739	609	635	381	1781	1803	2006	1416	1644	352
Case 3	5.04	995	1443	1358	611	635	381	1547	1607	1720	1263	1410	353
Case 4	3.64	996	972	966	611	635	381	1156	1260	1243	1007	1019	353
Case 5	3.13	997	651	838	612	635	381	1011	1122	1066	912	874	354
Case 6	2.15	997	573	587	611	635	381	740	850	736	735	603	353
Case 7	0.97	996	260	239	611	635	381	409	468	332	518	272	353

Note: 1 mm. = 1/25.4 in.; 1 MPa = 0.145 KSI.

Flexural Moment Envelop

The nominal flexural strength, M_n for any section can be calculated as a function of average developed strand stress, f_{dev} using ACI 318-14 [2] equation for moment capacity. The developed strand stress f_{dev} over the transfer length has been calculated using the formulation proposed by Brooks et al. [39] as shown in Eq. 24

$$\begin{aligned} f_{dev} &= \frac{x}{l_t} f_{se} && \text{where } x \le l_t \\ f_{dev} &= f_{se} + \frac{(x - l_t)}{l_b}(f_{ps} - f_{se}) && \text{where } l_t \le x \le l_d \\ f_{dev} &= f_{ps} && \text{where } l_d \le x \end{aligned} \tag{24}$$

Where, l_t has been calculated using Eq. 23 and the strand strain and slip obtained from the FEA results and l_b has been calculated using Eq. 25.(Brooks et al. [39])

$$l_b = 3\frac{(f_{pe} - f_{se})}{f_{se}} lt \quad \text{mm} \tag{25}$$

Fig 16 (a) shows the developed strand stress f_{dev} over the transfer length and the flexural bond length, both according to ACI 318-14 [2] (Eq. 2) and also as affected by excess initial slip according to the slip theory (Eq. 7). Fig 16 (b) shows the moment strength envelop, along with the external moment due to the applied load. It can be seen from figure 16 (b), the moment capacity is reduced in development length region due to excessive strand slippage. The results from the finite element analysis of the bridge girder shows that a bond failure would occur before the flexural failure at a strand slip of 3.13 mm.

By equating the transfer lengths from the slip theory [19] using constant bond stress hypothesis with the transfer length from ACI 318-14 [2] provisions, the allowable end slip $s_{allowable}$ can be calculated as given in Eq. 26.

$$s_{allowable} = 0.024 \frac{f_{se} f_{si} d_b}{E_p} \quad \text{mm} \tag{26}$$

Substituting values for E_p, f_{se}, f_{si}, d_b for the girder analysed in this study, gives the allowable end slip to be 2.2 mm (0.087 in.). Therefore, it can be concluded that the ACI theory transfer length is conservative when the allowable slip (for a particular value of f_{pe}, f_{si}, d_b and E_p) does not exceed 2.2 mm (0.087 in.). Similar observation has been reported by Brooks et al. [39] and Logan [40]. Brooks et al. [38] reported that, for prestress transfer length to be limited to the ACI recommendation (Eq. 2), the maximum allowable initial strand slip varies approximately between 1 mm (0.039 in.) to 3 mm (0.118 in.), depending upon strand diameter and levels of initial and final prestress. Similarly, Logan [40] reported that when the end slip was kept below, above or same as that of ACI allowable end slip of 2.2mm (0.087 in.), the nominal moment capacity M_n remains the same, but the transfer length and flexural bond length are decreased or increased compared to ACI recommendation (Eq. 2).

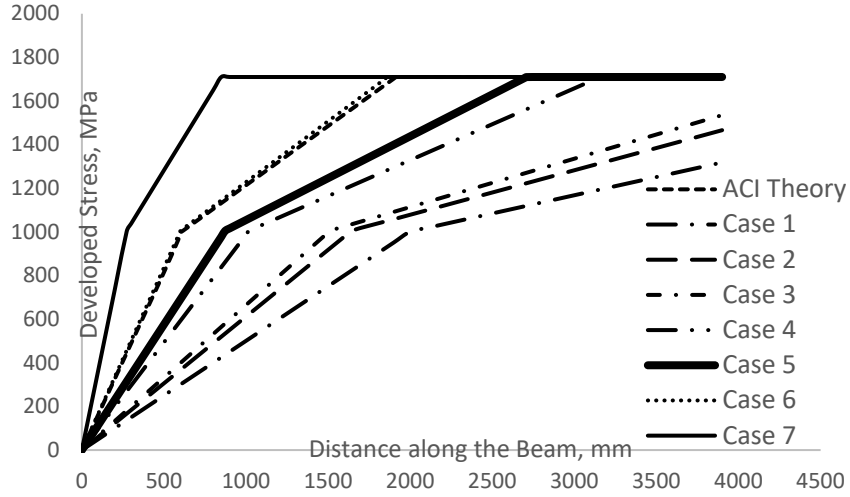

Fig 16 (a) Strand Stress Envelop Over Transfer Length and Flexural Bond Length

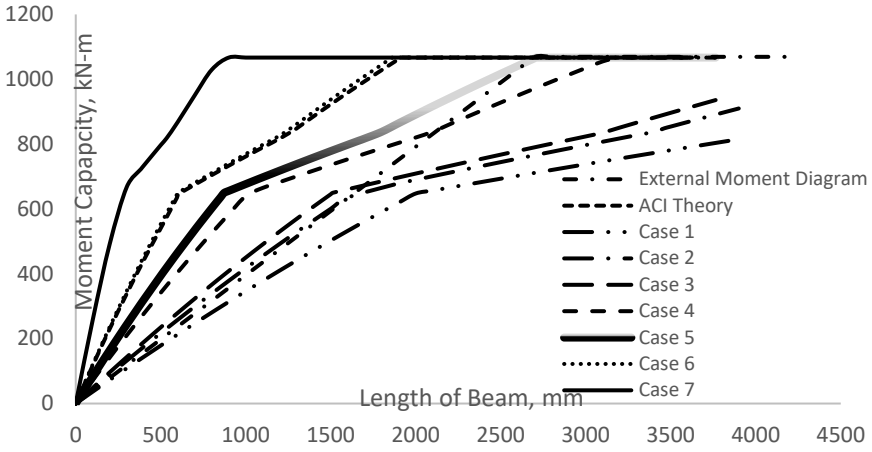

Fig 16 (b) Moment Envelop Over Transfer Length and Flexural Bond Length

CONCLUSION AND RECOMMENDATION FOR DESIGNERS

1. Surface roughness of strands considerably affects transfer length of prestressing strands. However there is no significant influence of the surface roughness on the effective prestress.
2. For prestress transfer length to be limited to the ACI 318-14 [2] transfer length value, the maximum allowable strand slip $s_{allowable}$ should be approximately 2.2 mm (0.087in.).

3. The developed stress f_{dev} and the moment capacity M_n predicted from the FEA results were higher than ACI theory in the development length region when the strand slippage was within the allowable strand slip.
4. The developed stress f_{dev} and the moment capacity M_n predicted from the analysis results were lower than the ACI theory in the development length region, when the strand slippage exceeded the allowable strand slip.
5. Excessive slippage of strands results in increase of transfer length, thus strand slipping should be considered as a quality control parameter in design of pre-tensioned members and suitable criteria should be developed that would give acceptable transfer length and end slip for specific applications.

From the finite element study it has been observed that excessive strand slip can result in codal violations for transfer length. It is thus recommended to field engineers that a standardized test, measuring the end slip of pretensioned strand after release should be developed and adopted to assess the excessive strand slippage and bond performance of pretensioned strand.

These conclusions are based on the study of the TxDOT Type-A bridge girders tested by Laskar et al. [25] for a particular set of parameters like, cross-section of the member, grade of concrete, grade of strand, diameter of tendon and initial and final prestress. Any change in parameters or cross-section of the bridge girder may need further study and verification.

REFERENCES

1. IS 1343-1984, “Code of Practice for Prestressed Concrete”, *Bureau of Indian Standards*, New Delhi, India, 1984.
2. ACI Committee 318, “Building Code Requirements for Structural Concrete (ACI 318-14) and Commentary (ACI 318R-14)” *American Concrete Institute*, Farmington Hills, MI, 2014.
3. AASHTO. Standard Specifications for Highway Bridges, 16th Edition, *American Association of State Highway Transportation Officials*, Inc., Washington, D.C., 1996.
4. Hanson N.W., Kaar P.H., “Flexural bond tests of pretensioned prestressed beams,” *In Journal Proceedings* V. 55, No. 1, January,1959, pp. 783-802.
5. Rose D.R., Russell B.W., “Investigation of standardized tests to measure the bond performance of prestressing strand,” *PCI journal*, V. 42, No.4, 1997 pp. 56-80
6. Balazs G.L., “Transfer control of prestressing strands.” *PCI journal*, V.37, No.6, November 1992, pp. 60-69.
7. José R., Vargas M., Cesar A., Pedro S.R., Carmen C.B., "Reliability of transfer length estimation from strand end slip." *ACI Structural Journal, V.* 104, No. 4, July 2007, pp. 487.
8. Hwan B., Lim S.N., Lee M.K., Yoo S.W., “Analysis and prediction of transfer length in pretensioned, prestressed concrete members.” *ACI Structural Journal*, V 111, No. 3, May 2014, pp 549.
9. Dang C.N., Floyd R.W., Hale W.M., Vargas M., “Measured Transfer Lengths of 0.7 in. (17.8 mm) Strands for Pretensioned Beams”, *ACI Structural Journal*, V. 113, No. 1, Jan 2016, pp. 85.
10. Janney J.R., “Nature of bond in pre-tensioned prestressed concrete.” *In Journal Proceedings*, V. 50, No. 5, May 1954, pp. 717-736.
11. Marin L.D., Scott N.L., “Development of Prestressing Strand in Pretensioned Members.” *In Journal Proceedings*, V. 73, No. 8, Aug 1976, pp. 453-456.
12. Galvez J.C., Benitez J.M., Casati M.J., Tork B.S., Cendon D.A., “Cohesive-frictional model for bond and splitting action of prestressing wire”. *International Journal for Numerical and Analytical Methods in Geomechanics*. V. 35 No. 11, August 2011,pp. 1257-1277
13. Moustafa S., "Pull-Out Strength of Strand and Lifting Loops," *Concrete Technology Associates Technical Bulletin*, May 1974, pp. 74-85.
14. Post-Tensioning Institute. "Recommendations for Prestressed Rock and Soil Anchors”. 2014.
15. Naito C., Cetisli F., Tate T., “A method for quality assurance of seven-wire strand bond in portland cement concrete.”, *PCI Journal*, July 2015, pp. 69-84.
16. Uijl J.A., “Bond modelling of prestressing strand”. *Special Publication*, V. 180, Oct 1998 , pp 145-70.
17. ASTM., “A416/A416M-10 standard specification for steel strand, uncoated seven-wire for prestressed concrete.” West Conshohocken, PA, *American Society for Testing and Materials*, 2010.
18. Anderson A.R., Anderson G.R, "An Assurance Criterion for Flexural Bond Pretensioned Hollow Core Units." *Journal Proceedings.* V. 73, No. 8. 1976.
19. Guyon Y., “Pretensioned Concrete: Theoretical and Experimental Study”, Paris, France, 1953, pp. 145-1701.
20. Bamonte P., Coronelli D., Gambarova P. G., "Local bond stress-slip law and size effect in high-bond bars." *Proc., 5th Int. Conf. on Fracture Mechanics of Concrete and Concrete Structures—FRAMCOS'5*, V. 2, 2004.
21. Stephen E., “Simulation of the long-term behaviour of precast/prestressed concrete bridges”, *Doctoral dissertation, University of Cincinnati*, 2006.

22. Kannel J., French C., Stolarski H., "Release methodology of strands to reduce end cracking in pretensioned concrete girders." *PCI journal*, V. 42, No. 1, 1997, pp 42-54.
23. Prashant M., Rajendhiran, Santhi A.S., "Behaviour of prestressed monoblock concrete sleeper under quasi-static loading." *International Journal of Innovative Engineering and Technology (IJSIET)*, Vol. 2, 2015.
24. ABAQUS. "ABAQUS software Version. 6.9". *Providence RI, USA: Dassault Systèmes Simulia Corp*, 2009.
25. Laskar A., Hsu T.T.C., Mo Y.L., "Shear Strengths of Prestressed Concrete Beams Part 1: Experiments and Shear Design Equations", *ACI Structural Journal*, V. 107. No.3, May-June 2010, pp 330-339.
26. Lee J., Fenves G, "Plastic-damage model for cyclic loading of concrete structures." *Journal of engineering mechanics*, V. 124, No. 8, 1998, pp 892-900.
27. Systemes, Dassault. "ABAQUS Analysis User's Manual Version 6.13." *Dassault Systemes Simulia, Providence*, 2013.
28. Carreira D. J., Chu K.H, "Stress-strain relationship for plain concrete in compression." *Journal Proceedings*, V. 82. No. 6, 1985, pp. 797-783.
29. Carreira D. J., Chu K.H, "Stress-strain relationship for reinforced concrete in tension". *In Journal Proceedings*, V. 83, No. 1, Jan 1986, pp. 21-28.
30. Wang, J., "Constitutive Relationships of Prestressed Concrete Membrane Elements," Ph.D. Dissertation, Department of Civil and Environmental Engineering, University of Houston, Houston, TX, August 2006.
31. AASHTO LRFD. "AASHTO LRFD bridge design specifications. 4th edition". *Washington, DC: American Association of State Highway and Transportation Officials*, 2007.
32. Eligehausen R., Egor P.P., Vitelmo V.B., "Local bond stress-slip relationships of deformed bars under generalized excitations.", 1982, pp 69-80.
33. Gan Y., "Bond stress and slip modeling in nonlinear finite element analysis of reinforced concrete structures." *PhD thesis University of Toronto*, 2000.
34. Herrero V., Martínez L.C., Aguilar G., Martínez A. F., "Evaluation of strand bond properties along the transfer length of prestressed lightweight concrete members." *Engineering Structures*, V. 49, 2013. pp 1048-1058.
35. Chen G., SEI F., Bao Y., "Development of Bridge Girder Movement Criteria for Accelerated Bridge Construction", No. NUTC R316, June 2014.
36. Russell B.W., Burns N.H., "Design guidelines for transfer, development and debonding of large diameter seven wire strands in pretensioned concrete girders." *final report*, Jan 1993.
37. Barnes W, Robert W., Burns N,. "Experimental assessment of factors affecting transfer length." *Structural Journal*, V. 100, no. 6, 2003, pp 740-748.
38. Cousins T.E, Badeaux M., Moustafa S., "Proposed test for determining bond characteristics of prestressing strand." *PCI Journal*, V. 37, No. 1, 1992, pp 66-73.
39. Brooks M., Gerstle K.H., Logan D.R, "Effect of Initial Strand Slip on the Strength of Hollow-Core Slabs." *PCI Journal*, V. 33, No. 1, 1988: pp 90-111.
40. Logan D. R., "Acceptance criteria for bond quality of strand for pretensioned prestressed concrete applications." *PCI journal*, V. 42, No. 2, 1997, pp 52-90.